

# EFFECT OF DIAPHRAGM FLEXIBILITY ON SEISMIC RESPONSE OF BUILDING STRUCTURES

Masayoshi Nakashima (I)  
Ti Huang (II)  
Le-Wu Lu (II)  
Presenting Author: Le-Wu Lu

## SUMMARY

This paper presents the diaphragm effect of RC floor slabs on building response. First, in-plane characteristics of RC floor slabs are investigated based upon experiment and finite element analysis. A model representing the in-plane hysteretic behavior of RC floor slabs is proposed. A building structure is analyzed for its earthquake response, and the diaphragm effect of floor slabs on the total base shear, base shear distribution to each frame, and the shear force distribution along the height is demonstrated.

## INTRODUCTION

When building structures are subjected to earthquake loadings, the induced inertial forces are transmitted through floor slabs and resisted by vertical structural components such as shearwalls and frames. In this situation, the floor slabs function as diaphragms placed between the vertical components. In analysis and design of three-dimensional structures under seismic loadings, the diaphragms frequently are assumed to be perfectly rigid. In certain types of structures, however, this assumption is found to create significant discrepancy on the lateral load distribution. This discrepancy frequently occurs in frame-wall structures, in which the vertical components consist of shearwalls with high story stiffnesses and relatively flexible frames. When there is a significant difference in story stiffness between two adjoined vertical members, the floor slab (diaphragm) connecting the members would sustain high in-plane shear. The high shear, in turn, would cause in-plane deformation of the floor slab. Buildings having a long and narrow floor plan (slender plan) have the same potential problem. In this type of buildings, floor slabs act like flexible beams, and bending deformation of the slabs becomes significant, referred to as the bowing action of the slab. In either type of structures, the actual distribution to vertical members could differ a great deal from the distribution obtained on the basis of the rigid assumption.

To study the effect of such diaphragm action of floor slabs on building response, first, this paper discusses in-plane characteristics of RC floor slabs, the most critical factor to control the diaphragm action, on the basis of the results of previously conducted experiments

- 
- (I) Research Engineer, Building Research Institute, Ministry of Construction, Ibaraki, JAPAN  
(II) Professor of Civil Engineering, Lehigh University, Bethlehem, Pennsylvania, USA

(Refs. 1 and 2) and finite element analysis, and proposes a model representing the in-plane hysteretic behavior of RC floor slabs. Second, a building structure is analyzed for its earthquake response. The proposed hysteresis model is incorporated into the analysis, and effects of the flexible diaphragm action on the building response are demonstrated.

## IN-PLANE CHARACTERISTICS OF RC FLOOR SLABS

### 3D Behavior vs. 2D Behavior

Since floor slabs sustain out-of-plane bending caused by vertical load even when they function as diaphragms, their diaphragm behavior is a combination of both the in-plane and out-of-plane loadings. The strict analysis, therefore, should include the complex interaction between those two types of loading. In the previous experiments (Refs. 1 and 2), many pairs of RC floor panels were tested for their diaphragm behavior, one without vertical load, the other with out-of-plane force corresponding to the sum of the dead weight and the service live load. Comparison of the results showed that the basic behavior of the two floor panels was approximately the same; the crack pattern, failure mode, and stiffness degradation behavior were almost identical; and the difference in the ultimate load was not more than 15 percent. Based on those observations, it was assumed that the diaphragm behavior of a floor slab is represented by its behavior under in-plane force only. With this assumption, the analysis of floor slabs as diaphragms is simplified to the two dimensional plane stress problem.

### Finite Element Analysis

A 2D plane stress nonlinear finite element model was developed to extend the investigation of the in-plane characteristics of RC floor slabs. The basic analytic procedures of this model are as follows: the constitutive relationship devised by Darwin (Ref. 3) was used for representing the concrete behavior. Reinforcing steel was idealized as an orthotropic material with bi-linear stress strain relationship. Effect of bond slip was not included. The finite element used in the analysis was a four noded isoparametric quadrilateral with four extra nonconforming modes. The nine point Gaussian integration scheme was used to form stiffness matrices. The solution was derived through iterations in order to reflect material nonlinearities of concrete and steel.

The ability of the model to simulate the in-plane behavior of floor slabs was demonstrated by analyzing three floor panels (designated as Cases 1 to 3) tested in Refs. 1 and 2. Figure 1 shows the basic part of the tested floor panels. Following the loading and support conditions employed in the test, in this analysis, one of the longer edges was clamped, while the other three are stress free. Shear force (and bending moment in two cases) was applied proportionally at the edge opposite to the clamped edge. The basic panel was discretized as shown in Fig. 2. The basic load conditions and material properties used in the analysis are listed in Tables 1 and 2. Figure 3 shows the load vs. deflection curves of these panels obtained from the analysis and from the tests. The

analytical model can duplicate the experimental load vs. deflection curves satisfactorily.

#### Strength Characteristics

Using the finite element model, a variety of floor panels were analyzed for their in-plane behavior. The major variables in this parametric analysis were the arrangement of reinforcement and the moment-to-shear ratio in in-plane loading. Table 3 tabulates the reinforcement and loading conditions and the results of the analyzed floor panels. In all cases, the floor panel having beams and the dimensions and support conditions in Fig. 1 was analyzed, and for the arrangement of reinforcement, the one used in the experiment was taken as the standard since it was designed according to the present ACI code.

The results showed that there are essentially two types of failure mode: one the flexural failure, the other the (inclined) shear failure. For the flexural failure, the critical section (where a hinge was formed) was either the clamped edge of the panel at which the largest moment was applied or the boundary between the column and middle strips at which some negative reinforcement was terminated. In either case, it was found that the ultimate in-plane shear can be well estimated simply by dividing the flexural capacity of the critical section by the shear span length (See Table 3). In cases when the reinforcement parallel to the loading (serving as the shear reinforcement) is little relative to the flexural reinforcement, the panel exhibited shear failure. It was also found that the failure force can be estimated reasonably with use of the ACI code formula (11.3.1.1) offered for computing the shear force carried by cracked concrete (Table 3).

#### Initial In-Plane Stiffness

Using this model, the initial (uncracked) stiffness of floor panels was examined with the moment-to-shear ratio of the floor panel and the relative beam size as parameters. The loading and support conditions followed those in Fig. 1. The relative beam size was defined as in Fig. 4. Based upon the results, a validity of estimating the initial in-plane stiffness of floor slabs by treating the floor panel as a deep beam was calibrated. First, the effective moment of inertia of the beam ( $I_e$ ) was estimated from the shear and end rotation (that of the free edge) obtained in the analysis and the force vs. end rotation relationship given by the simple beam theory. Using thus obtained  $I_e$  and again the beam theory, the end deflection caused by the flexure (assumed) was calculated. The difference between this flexural deflection and the total end deflection obtained in the analysis was taken as the shear deflection. The effective shear area of the deep beam ( $A_e$ ) was estimated from this shear deflection and the shear force vs. shear deflection relationship given by the beam theory.

Major findings in this calibration are as follows. The values of  $I_e$  are very close to the nominal moment of inertia of the floor panel regardless of the moment-to-shear ratio or the relative beam size, while the values of  $A_e$  are affected by these variables. For practical evaluation, nevertheless, the cross sectional area of the panel (not

including the area of beams) can represent reasonably well the shear area. This simplification results in an error of less than 12 percent in the shear deflection for the moment-to-shear ratios and relative beam sizes covered in this study. The analysis also proved that the stiffness starts degrading once a flexural crack occurs in the panel.

#### Inelastic (Cracking) In-Plane Stiffness

An attempt was made to extend this deep beam analogy to the stiffness evaluation in the inelastic (cracked) range. In order to reflect the stiffness degradation in this range, hypothetical flexural and shear stiffnesses, referred to as the equivalent flexural stiffness  $(EI)_e$  and the equivalent shear stiffness  $(GA)_e$ , were introduced respectively. The procedure to estimate those equivalent stiffnesses was identical to that to compute  $I_e$  and  $A_e$  in the initial stiffness range. Employing the experimental and analytical results (these tabulated in Table 3) in this analogy, the estimated flexural and shear deflections are plotted as the relative deflection in Fig. 5. Two interesting phenomena can be noted from this figure. First, the proportion in relative deflection remains relatively the same regardless of the load level for all of the examined floor panels. Second, the proportion matches the elastic proportion: the proportion computed from the elastic formulas and denoted by the dot lines in Fig. 5. These findings confirm that both the flexural and shear stiffnesses degrade proportionally regardless of the loading and support conditions, or the load level. Once the ratio of the equivalent flexural (shear) stiffness at a given load level to the initial flexural (shear) stiffness is known, the in-plane stiffness at this load level can be determined simply by multiplying the elastic stiffness by this ratio.

#### Hysteresis Model of RC Floor Slabs

An in-plane hysteresis model of RC floor slabs is now developed base upon the findings in the previous section. First, it is assumed that the floor panel fails in flexure mode, and after reaching the ultimate load, the panel exhibits stable plastic behavior. Such behavior can be achieved if the panel is properly reinforced against shear. The second assumption, already verified in the previous section, is that the shear stiffness decreases in proportion to the flexural stiffness in the inelastic region. Cracking force is estimated as the force when the largest moment applied to the panel causes a specified strain at the tension edge with the strain computed according to the assumption that a plane section remains plane. Until the cracking moment reaches, the panel is assumed to hold its initial stiffness. Once cracking occurs, the flexural stiffness is assumed to decrease by a reduction factor and remain constant until the maximum moment reaches. This reduction factor is taken as the ratio of the slope defined by connecting the cracking and maximum moment points to the initial slope in the moment curvature diagram of the critical section of the floor panel. (See Fig. 6) When load reversal occurs, the force is assumed to decrease linearly with deflection, shooting the origin. This is the last assumption, and adopted by examining the experimentally obtained hysteresis loops. This origin oriented hysteresis produces no energy dissipation as long as the succeeding loading does not exceed the

previously obtained maximum deflection. Since RC floor slabs are lightly reinforced with respect to the diaphragm behavior, this assumption should be reasonable. Figure 7 illustrates the proposed in-plane hysteresis model for RC floor panels in terms of the largest moment applied to the panel and the end rotation.

## DIAPHRAGM EFFECT IN BUILDING RESPONSE

### Building Model and Analysis

A reinforced concrete building model with seven stories, six bays in width, and one bay in depth was selected for the analysis. Figure 8 illustrates the plan and elevation views of this building and its critical dimensions. The ground acceleration was applied to the direction perpendicular to the longer horizontal direction of the structure. This structure has a relatively slender plan section, whose aspect ratio is 1 : 6. This dimension was chosen intentionally so that the floor slabs would play a significant role on the distribution of lateral force to vertical elements. As discussed earlier, a slender plan tends to amplify the bending action of floor slabs. In addition, a great difference in lateral stiffness between adjoined vertical elements increases the force to be transmitted through the floor slab connecting these components. This increase in force may cause severe distortion of the floor slab.

For the dynamic analysis, the structure was simplified to a discrete model (Fig. 9). In this model, all structural components: floor slabs, frames, and walls, were simplified to flexural line elements. To represent the restoring force characteristics of the floor slabs, the model proposed in the previous section was employed. The frame and shear wall behavior was represented by the degrading tri-linear model devised by Clough and Johnston. For frames, the model was used to define the shear force vs. story deflection relationship, and no interaction in hysteretic characteristics between stories was considered. For shearwalls, the interaction was taken into account by adopting the rules as defined for floor slabs. Shear deflection was included in the floor slabs and shearwalls by using the assumption that the shear stiffness degrades in proportion to the flexural stiffness. Mass and other major properties used in the analysis are listed in Table 4. The Newmark Method (with  $\beta = 1/4$ ) was used in the direct integration, and the record of the N-S component of EL Centro Earthquake (1940) was selected as the input ground motion with 0.33 g of the maximum acceleration.

### Results and Discussions

The model structure was analyzed for the following three cases (Cases 1 to 3): Case 1: linear elastic analysis with the rigid slab assumption, Case 2: linear elastic analysis and Case 3: nonlinear analysis. The results including the maximum displacement, acceleration, and base shear to each vertical element are tabulated in Table 5. Comparing the three numerical results, diaphragm effects of the floor slabs on the earthquake response of the model building can be summarized as follows.

- 1) Inclusion of diaphragm flexibility changed little the natural period of the structure and the maximum total base shear. Difference in the base shear was not more than 8 percent.
- 2) The rigid slab assumption caused significant underestimate of the base shear resisted by the frames. The base shear in the middle frame (Frame 3 in Fig. 8) was reduced only to 23 percent if the rigid assumption was adopted.
- 3) The floor slabs reached their maximum moments at the junction with Frame 3 in the nonlinear analysis. On the other hand, the maximum shear force applied to the floor slabs was 0.37 MN, which was less than 50 percent of the force computed by the ACI code formula 11.3.1.1, 1.05 MN, which specifies the nominal shear strength provided by concrete. In the model structure, the flexural behavior of the floor slabs controlled the diaphragm action.
- 4) Nonlinear action of the structural components changed both the base shear distribution to the frames and shearwall (Table 5) and the effective earthquake force distribution over the height of these components. The total earthquake force applied to each story was distributed approximately in the inverted triangular fashion along the height, but the distribution in each frame or shearwall was by no means inverted triangular.

#### REFERENCES

1. Karadogan, H.F., et al., "Behavior of Flat Plate Floor Systems Under In-Plane Seismic Loading," Proceedings, 7WCEE, Vol. 5, Turkey, pp.9-16.
2. Nakashima, M., Huang, T., and Lu, L. W., "Experimental Study of Beam-Supported Slabs Under In-Plane Loading," ACI Journal, Vol. 79, No. 1 Jan/Feb 1982, pp.59-65.
3. Darwin, D., "Inelastic Model for Cyclic Biaxial Loading of Reinforced Concrete," Ph. D. Dissertation, Dept. of Civil Engineering, University of Illinois at Urbana-Champaign, 1974, 170p.

Table 1 Analyzed Floor Panels

Case	Panel	Type of Slab	Thickness	Loading Condition
1	middle	flat slab	56.4 mm	shear and moment
2	middle	slab on beam	39.5 mm	shear and moment
3	right	slab on beam	39.5 mm	shear

Table 2 Material Properties of Analyzed Floor Panels

		Case 1	Case 2	Case 3
Steel	Yield stress (MPa)	415	368	368
	Modulus of elasticity (GPa)	198	191	191
	Strain hardening modulus	1/300 times initial		
Concrete	Uniaxial comp. strength (MPa)	32	29.5	28
	Uniaxial tensile strength (MPa)	3.5	3.5	2.5
	Initial modulus (GPa)	24	22	22
	Strain corresponding to maximum compressive strength (m/m)	-.0023	-.0024	-.0024
	Poisson's ratio	0.2		

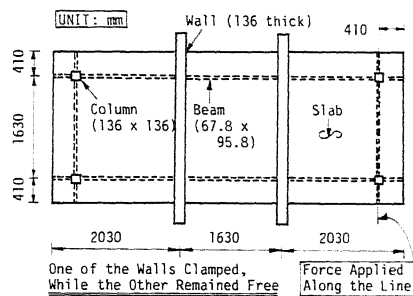


Fig.1 Tested Floor Panel and its Dimensions (Refs.1 and 2)

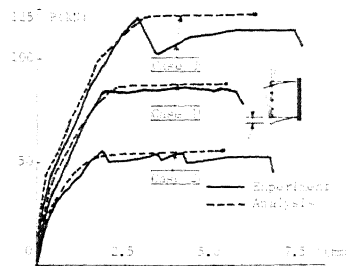


Fig.3 Comparison between Test and Analysis

Table 3 Parameters of Analyzed Panel and Results

Case	Moment-to-Shear Ratio	Slab Reinforcement		Beam Reinforcement	Failure Mode	Maximum Load	Maximum Load Based on Flexural Capacity
		Flexure	Shear				
1	1.63 m	S	S	S	F	118 kN	125 kN
2	3.25 m	S	S	S	F	52 kN	54 kN
3	6.51 m	S	S	S	F	31 kN	34 kN
4	infinity	S	S	S	F	150 kN	155 kN
5	0.812 m	S	S	S	SH	120 kN	340 kN
6	0.0 m	S	S	S	SH	112 kN	-
7	1.63 m	double	S	S	SH	131 kN	239 kN
8	1.63 m	S	S	double	SH	125 kN	280 kN
9	1.63 m	S	double	S	F	211 kN	125 kN

NOTATION: S: standard, F: Flexural Failure, SH: Shear Failure

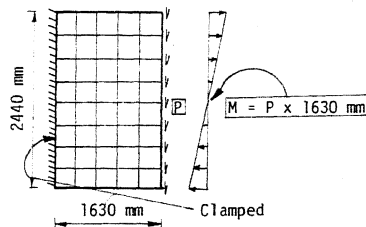


Fig.2 Discretization of Analyzed Floor Panel

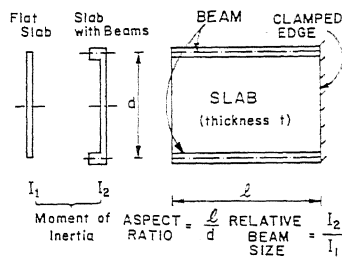


Fig.4 Initial Stiffness Evaluation

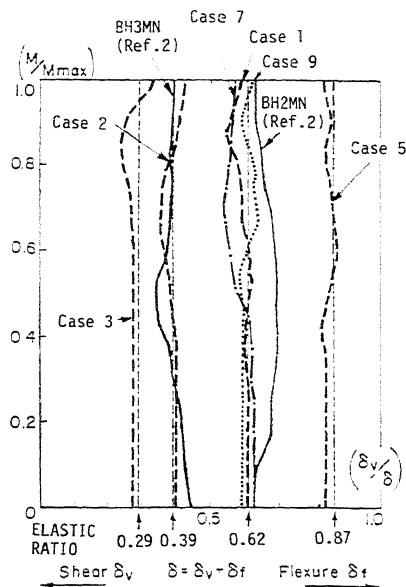


Fig.5 Ratio of Flexural and Shear Deflections

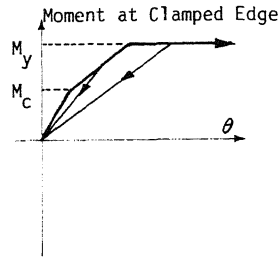
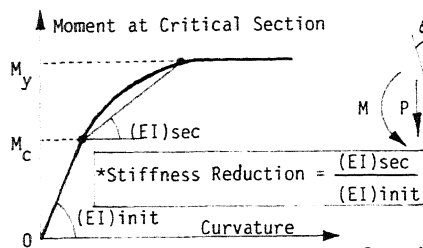


Table 4 Mass and Other Properties Used in Analysis

	Moment of Inertia	Shear Area	Maximum Moment	Ratio of $M_c$ to $M_y$	Ratio of $E_{is}$ to $E_{li}$	Mass	Span			
slab	3.63	1.08	2.94	0.30	0.13	7th	30.1	37.3	37.3	18.6
wall	5.79	1.60	24.5	0.41	0.21	6th	30.1	37.3	37.3	18.6
						5th	30.1	37.3	37.3	18.6
						4th	30.1	37.3	37.3	18.6
						3th	30.1	37.3	37.3	18.6
						2nd	30.1	37.3	37.3	18.6
						1st	31.9	38.0	38.0	19.0
frame (1st st.)	108 MN/m		0.867 MN	0.25	0.18					
frame (others)	211 MN/m		1.08 MN	0.25	0.18					

UNIT: Moment of Inertia =  $m^4$ , Shear Area =  $m^2$ , maximum Moment = MN x m, Mass = kg  
 NOTATION:  $M_c$  = Cracking Moment (Shear),  $M_y$  = Maximum Moment (Shear)  
 $E_{is}$  = Inelastic Stiffness,  $E_{li}$  = Initial Stiffness

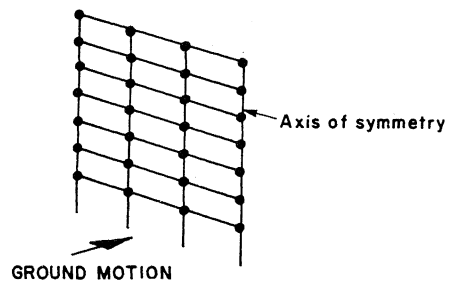
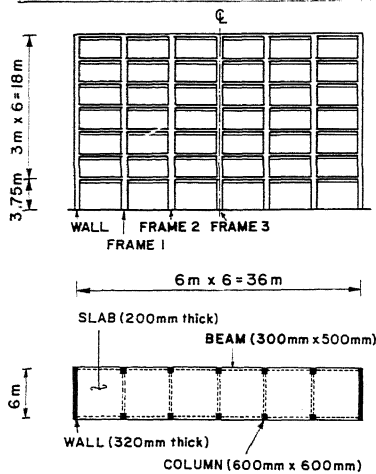


Table 5 Results of Dynamic Response Analysis

Case	Maximum Disp.	Maximum Accel.	Total Base Shear	Base Shear to Each Element (MN)			
1	29.6 mm	10.0 m/sec <sup>2</sup>	7.29 MN	Wall	Frame 1	Frame 2	Frame 3
2	34.2	9.74	8.24	3.34	0.119	0.119	0.119
3	72.5	12.5	8.05	3.16	0.322	0.462	0.515
				2.23	0.867	0.867	0.867

Max. disp. and accel. are those at 7th story of Frame 3 (middle frame)